

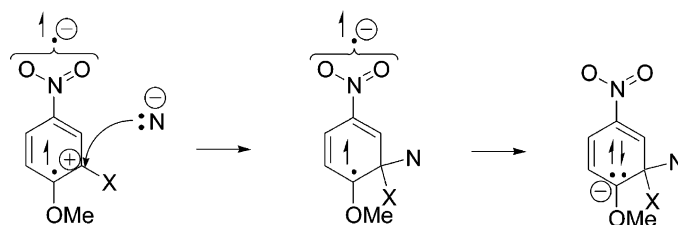
## The Element Effect and Nucleophilicity in Nucleophilic Aromatic Photosubstitution ( $S_N2Ar^*$ ). Local Atom Effects as Mechanistic Probes of Very Fast Reactions

Gene G. Wubbels,\* Toby R. Brown, Travis A. Babcock, and Kandra M. Johnson

Department of Chemistry, University of Nebraska at Kearney, Kearney, Nebraska 68849

wubbelsg@unk.edu

Received November 17, 2007



Photoreactions of 4-nitroanisole and the 2-halo-4-nitroanisoles (halogen = F, Cl, Br, and I) with the nucleophiles hydroxide ion and pyridine have been investigated quantitatively to extend the findings recently communicated for cyanide ion. The halonitroanisoles on excitation form triplet  $\pi, \pi^*$  states, which undergo substitution of the halogen by nucleophiles. Chemical yields of photoproducts, Stern–Volmer kinetic plots, triplet lifetimes, and triplet yields are reported for the five compounds with the three nucleophiles. Following a standard kinetic treatment, 73 rate constants are determined for elementary reactions of the triplets including quenching and various nucleophilic addition processes. The photoadditions are roughly 14 orders of magnitude faster than thermal counterparts. Rate constants for attack at the fluorine-bearing carbon of triplet 2-fluoro-4-nitroanisole are  $2.9 \times 10^9$ ,  $1.3 \times 10^9$ , and  $6.3 \times 10^8 \text{ M}^{-1} \text{ s}^{-1}$  for cyanide ion, hydroxide ion, and pyridine, respectively. The relative rates for attack at the halogen-bearing carbons for F/Cl/Br/I are 27:1.9:1.9:1 (cyanide ion), 29:2.6:2.4:1 (hydroxide ion), and 39:3.9:3.5:1 (pyridine), respectively. The relative nucleophilicities vary somewhat with the attack site; they are about 5:2:1 for cyanide ion, hydroxide ion, and pyridine for attack at the halogen-bearing carbons. The trend of the element effect opposes that of aliphatic substitution and elimination but is similar in size and parallel to that of thermal nucleophilic aromatic substitution. Relative nucleophilicities in the photoreactions are also similar to those of comparable but vastly slower thermal reactions. The findings imply that the efficiency-determining step of the halogen photosubstitution is simple formation of a  $\sigma$ -complex through electron-paired bonding within the triplet manifold.

### Introduction

Important aspects of the mechanism of nucleophilic aromatic photosubstitution of the  $S_N2Ar^*$ -type reaction remain unclear. These reactions, whose mechanisms<sup>1,2</sup> and applications<sup>3,4</sup> have been studied extensively, are generally agreed to involve an

intermediate singlet  $\sigma$ -complex,<sup>5</sup> but there is little evidence for the  $\sigma$ -complex. It occurred to us that this mechanism could be studied definitively by use of the element effect of halogens and relative nucleophilicities. Photochemists have made little mechanistic use of local substituent effects, possibly because of the limitation that substituent changes must little affect the chromophore and its photophysics. Avoidance of such perturba-

(1) Terrier, F. *Nucleophilic Aromatic Displacement: The Influence of the Nitro Group*; VCH Publishers: New York, 1991; Chapter 6.

(2) Karapire, C.; Icli, S. In *Organic Photochemistry and Photobiology*, 2nd ed.; Horspool, W., Lenci, F., Eds.; CRC Press: Boca Raton, FL, 2004; Chapter 37, pp 37-1–37-14.

(3) Specht, A.; Goeldner, M. *Angew. Chem., Int. Ed.* **2004**, *43*, 2008.

(4) Schutt, L.; Bunce, N. J. In *Organic Photochemistry and Photobiology*, 2nd ed.; Horspool, W., Lenci, F., Eds.; CRC Press: Boca Raton, FL, 2004; Chapter 38, pp 38-1–38-18.

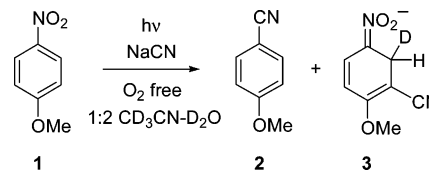
(5) Cornelisse, J.; Havinga, E. *Chem. Rev.* **1975**, *75*, 353.

tion with variation of the nucleofuge, as well as the nucleophile, seemed possible for the case of  $S_N2Ar^*$  reactions.

The element effect is a named entity in physical organic chemistry.<sup>6</sup> It refers to rate ratios in a reaction having reactants substituted with different atoms of the same group of the Periodic Table. The element effect, especially of the halogens, has played a fundamental role in resolving mechanisms in organic chemistry. The effect was central in understanding aliphatic substitution and elimination reactions<sup>7</sup> and nucleophilic aromatic substitution reactions of the  $S_N2Ar$  type.<sup>8,9</sup> It seemed possible at the least that we could establish whether the efficiency-determining transition state of the photosubstitution was dominated by leaving group effects as in thermal aliphatic substitution and elimination ( $F \ll Cl < Br < I$ ) or by  $\sigma$ -bond polarization and steric effects as in thermal nucleophilic aromatic substitution ( $F \gg Cl > Br > I$ ).<sup>10</sup> That we know little about relative nucleophilicity in photoreaction mechanisms may result from having discovered few reactions in which nucleophilic attack occurs directly on the excited-state molecule. Since nucleophilicity reflects local atomic and molecular properties independent of the photophysics of the substrate, this also seemed an auspicious probe.

Two models with different theoretical bases rationalize the regioselectivity of the  $S_N2Ar^*$  reaction,<sup>11,12</sup> but neither provides insight about the occurrence of the  $\sigma$ -complex that both assume or the proximate transition states. The transition state postulated for  $S_N2Ar^*$  reactions of nitrophenyl ethers involves formation of a  $\sigma$ -complex from attack of a nucleophile on a triplet  $\pi, \pi^*$  excited state.<sup>5</sup> This postulate, however, leaves several questions open. Complexes<sup>5</sup> or exciplexes<sup>13,14</sup> have been suggested to result from the encounter of excited state and nucleophile on the basis of some transient spectroscopy studies, while other studies<sup>15,16</sup> have found no need for exciplexes. Indeed, another mechanism, named  $S_N(ET)Ar^*$ ,<sup>1</sup> features a different transition state involving electron transfer from nucleophile to excited state.<sup>17–19</sup> It entails para-to-nitro regioselectivity for substitution, but several cases with amine nucleophiles have been shown likely to proceed by the  $S_N2Ar^*$  mechanism involving a fast sigmatropic rearrangement of a meta  $\sigma$ -complex to a para  $\sigma$ -complex.<sup>20</sup> The transition state for  $S_N2Ar^*$  mediates the fastest nucleophilic reactions known ( $k \approx$

### SCHEME 1. Photoproducts of 1 with Cyanide Ion under Oxygen-Free Conditions



$10^9 \text{ M}^{-1} \text{ s}^{-1}$ ); they are roughly  $10^{14}$  times faster than their thermal counterparts. The influence of local structural and electronic effects of substituents and of nucleophilicity on such fast substitution reactions has not been assessed. Moreover, the reaction from the excited state plus nucleophile to the  $\sigma$ -complex involves a large release of energy<sup>12</sup> and an electron spin inversion. The effect, if any, of the spin inversion on the rate has also not been established.

Establishing the halogen element effect and relative nucleophilicities for the elementary rate constants of a suitable series of photosubstitution substrates promised to answer several of these questions. The 2-halo-4-nitroanisole series seemed likely to suffice because the spectroscopy and photophysics are dominated by the nitrophenyl ether chromophore, efficiently giving a triplet  $\pi, \pi^*$  state on photoexcitation<sup>13–16</sup> that would be expected to be little affected by halogen substitution. Moreover, Havinga and co-workers had shown<sup>5</sup> that several 2-halo-4-nitroanisoles undergo photosubstitution of the halogen by hydroxide ion.

### Results

Photolyses of 4-nitroanisole (**1**) with cyanide ion in mixed aqueous solutions were carried out by Letsinger and co-workers.<sup>21</sup> They reported a nitrite displacement product and products resulting from bond formation by cyanide ion meta to the nitro group. When the photolysis medium was free of oxygen, they observed an intensely absorbing photoproduct of unknown structure that was stable in solution ( $\lambda_{\text{max}} = 364 \text{ nm}$  in 20% *t*-butyl alcohol/water). When we irradiated **1** in oxygen-free 33%  $\text{CD}_3\text{CN}-\text{D}_2\text{O}$  (v/v) containing NaCN at 313 nm at 0 or 35 °C, we found <sup>1</sup>H NMR evidence for two photoproducts (**2** and **3**) that accounted for 26 and 74%, respectively, of the reacted starting material. The results appear in Scheme 1. Compound **2** was expected<sup>21b</sup> and was confirmed with an authentic sample. The structure of nitronate ion **3** was inferred from its spectra. It showed  $\lambda_{\text{max}} = 371 \text{ nm}$  ( $\epsilon \approx 13\,000$ ) in 33%  $\text{CH}_3\text{CN}-\text{H}_2\text{O}$  and <sup>1</sup>H NMR signals (33%  $\text{CD}_3\text{CN}-\text{D}_2\text{O}$ ) as follows (shifts relative to  $\text{CD}_2\text{HCN}$  at  $\delta$  2.03):  $\delta$  6.56, 1H, d ( $J = 5.7 \text{ Hz}$ );  $\delta$  6.11, 1H, d ( $J = 5.7 \text{ Hz}$ );  $\delta$  3.79, 3H, s;  $\delta$  3.70, 1H, br s. When 3,5-dinitrobenzoic acid, a substance known to oxidize dihydrobenzenes to benzenes,<sup>22</sup> was added to the solution of **2** and **3** at 25 °C, the NMR signals of **3** were replaced slowly by those of 2-methoxy-5-nitrobenzonitrile with the C-6 position about 80% deuterated. That a nitronate ion is a stable photoproduct of **1** with the nucleophile, cyanide ion, is without precedent.

The photolyses of the 2-halo-4-nitroanisoles (**4** (2-F), **5** (2-Cl), **6** (2-Br), and **7** (2-I)) with cyanide ion were carried out

(6) Mueller, P. *Pure Appl. Chem.* **1994**, *66*, 1077.

(7) Lowry, T. H.; Richardson, K. S. *Mechanism and Theory in Organic Chemistry*, 3rd ed.; Harper & Row: New York, 1987; p 374.

(8) Bunnett, J. F.; Garbisch, E. W.; Pruitt, K. M. *J. Am. Chem. Soc.* **1957**, *79*, 385.

(9) Bordwell, F. G.; Hughes, D. L. *J. Am. Chem. Soc.* **1986**, *108*, 5991.

(10) A preliminary report of the element effect in photosubstitution by cyanide ion has appeared: Wubbels, G. G.; Johnson, K. M.; Babcock, T. A. *Org. Lett.* **2007**, *9*, 2803.

(11) Epiotis, N. D.; Shaik, S. *J. Am. Chem. Soc.* **1978**, *100*, 29.

(12) van Riel, H. C. H. A.; Lodder, G.; Havinga, E. *J. Am. Chem. Soc.* **1981**, *103*, 7257.

(13) Varma, C. A. G. O.; Tamminga, J. J.; Cornelisse, J. J. *Chem. Soc., Faraday Trans. 2* **1982**, *78*, 265.

(14) van Eijk, A. M. J.; Huizer, A. H.; Varma, C. A. G. O.; Marquet, J. *J. Am. Chem. Soc.* **1989**, *111*, 88.

(15) van Zeijl, P. H. M.; van Eijk, L. M. J.; Varma, C. A. G. O. *J. Photochem.* **1985**, *29*, 415.

(16) Bonhila, J. B. S.; Tedesco, A. C.; Nogueira, L. C.; Diamantino, M. T. R. S.; Carreiro, J. C. *Tetrahedron* **1993**, *49*, 3053.

(17) Yokoyama, K.; Nakamura, J.; Mutai, K.; Nagakura, S. *Bull. Chem. Soc. Jpn.* **1982**, *55*, 317.

(18) Wubbels, G. G.; Snyder, E. J.; Coughlin, E. B. *J. Am. Chem. Soc.* **1989**, *110*, 2543.

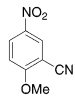
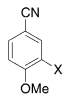
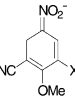
(19) Wubbels, G. G.; Ota, N.; Crosier, M. L. *Org. Lett.* **2005**, *7*, 4741.

(20) Wubbels, G. G.; Johnson, K. M. *Org. Lett.* **2006**, *8*, 1451.

(21) (a) Letsinger, R. L.; McCain, J. H. *J. Am. Chem. Soc.* **1969**, *91*, 6425. (b) Letsinger, R. L.; Hautala, R. R. *Tetrahedron Lett.* **1969**, 4205.

(22) Wubbels, G. G.; Halverson, A. M.; Oxman, J. D.; DeBruyn, V. H. *J. Org. Chem.* **1985**, *50*, 4499.

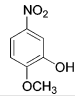
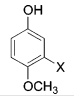
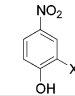
**TABLE 1.** Product Percent Yields from Photoreactions of 4–7 with NaCN by NMR Analysis

reactant			
4	88%	9%	3%
5	61%	29%	10%
6	57%	32%	11%
7	48%	43%	9%

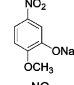
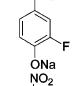
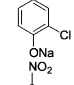
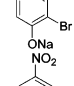
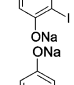
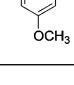
typically at 0.003 M with 0.01 M NaCN in oxygen-free 33% CD<sub>3</sub>CN/D<sub>2</sub>O (v/v) in NMR tubes at ca. 35 °C with unfiltered broad-band light at 300 nm. The methoxy singlets of photoproducts showed baseline separations at 300 MHz in the range of 4.0–3.6  $\delta$ . Integration of these signals, and the respective downfield signals in most cases, allowed yield estimations. Replacement of halogen by cyanide was the major reaction for 4–7, giving in all cases 2-methoxy-5-nitrobenzonitrile, whose methoxy peak is downfield 0.06 ppm from that of the starting materials. Its spectrum was confirmed with an authentic sample. A minor product resulted from nitro group displacement by cyanide, which gave a 0.06 ppm upfield-shifted methoxy signal relative to starting materials in all cases. These were confirmed with authentic samples for the chloride and bromide. The other minor product was the cyanide nitronate adduct analogous to 3, which showed in all cases a substantially upfield-shifted methoxy signal. This was confirmed for the chloride by oxidizing the solution containing the nitronate with 3,5-dinitrobenzoic acid, which caused the spectrum of 2-methoxy-3-chloro-5-nitrobenzonitrile to appear (deuterated at C-6). The product distributions were measured in duplicate at 20–40% conversion. The results are given in Table 1.

The photolyses of 1 and 4–7 with hydroxide ion were carried out as above but with NaOH at 0.01 M. The products were analyzed by NMR, but this analysis was inferior to a UV/vis analysis described below. The photolyses of 1 at 3 and 26 °C with hydroxide ion in aqueous media are reported<sup>23</sup> to give 4-methoxyphenol (80%) and 4-nitrophenol (20%). The products and yields from 1 with NaOH under our conditions in 33% CD<sub>3</sub>CN/D<sub>2</sub>O were the same. The photolyses of 4–7 with hydroxide ion gave in all cases 2-methoxy-5-nitrophenol as the major product. Quantification of this product was done by <sup>1</sup>H NMR integration using the entire spectrum, but especially the methoxy peak about 0.2 ppm upfield from that of the starting materials. Displacement of the methoxy group of 4–7 gave a minor product (2-halo-4-nitrophenol) in all cases plus methanol, whose singlet appeared 0.7 ppm upfield of the methoxy signal of starting materials. Here also, the entire spectrum was used for quantification except for the case of 4, where the downfield signals were too weak for accurate analysis. The spectra of the methoxy displacement products and methanol were confirmed with authentic samples. Displacement of the nitro group also gave rise to minor photoproducts, the 3-halo-4-methoxyphenols. This was shown by the coincidence of the spectrum of authentic 3-bromo-4-methoxyphenol with a minor product from the

**TABLE 2.** Product Percent Yields from Photoreactions of 4–7 with NaOH by NMR Analysis

reactant			
4	94%	3%	3%
5	70%	15%	15%
6	66%	16%	18%
7	62%	11%	27%

**TABLE 3.** UV/Vis Properties in 33% CH<sub>3</sub>CN/H<sub>2</sub>O, 0.0050 M NaOH of Photoproducts of 4–7 with NaOH for Quantitative Product Analysis

compound	$\lambda_{\max}$ , nm	$\epsilon$ at $\lambda_{\max}$	$\epsilon$ at 405 nm	$\epsilon$ at 323 nm	$\epsilon$ at 265 nm
	423 323 265 230	3740 5005 12600 9960	3510	5005	12580
	401 233	19060 5000	18750	1500	2500
	402 269 233	19250 3500 5200	18950	1000	3400
	404 270 232	19730 3800 5200	19560	1000	3400
	407 276 232	18980 4600 8300	18750	1800	3500
	302 233	2230 6200	0	1000	600

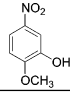
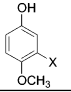
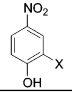
photoreaction of 6. The other photoproduct 3-halo-4-methoxyphenols showed almost identical spectra. Quantitative analysis of these products by NMR was problematic, however, especially for the halonitroanisoles that reacted less efficiently. The 3-halo-4-methoxyphenols were photolabile in alkaline 33% CD<sub>3</sub>CN/D<sub>2</sub>O. Photolysis of 3-bromo-4-methoxyphenol in alkaline solution caused photohydrolysis of the methoxy group, giving methanol, a photoreaction that has preceded.<sup>5</sup> The secondary photolysis frustrated the determination of yields of the minor products from the substances that reacted less efficiently. In those cases, the methanol signal was disregarded, and we used integrations of the weak downfield NMR signals at early conversions for specific minor products. We judge the results in Table 2 to be quite reliable for 4–6 but uncertain for the minor products of 7.

Because of the uncertainty, another method of analysis with quantitative UV/vis spectra was developed. Extinction coefficients were measured carefully for authentic samples of the photoproducts, and spectral overlays (200–600 nm) were made for each of the photoreactions of 4–7 with hydroxide ion, all in 33% acetonitrile/water. All photoreactions were carried to completion, and they showed sharp isosbestic points. The electronic spectra used are in Table 3.

The UV/vis analysis was rather blind to the secondary photochemistry of the 3-halo-4-methoxyphenols because their extinctions and those of their photoproducts are small relative

(23) Letsinger, R. L.; Ramsay, O. B.; McCain, J. H. *J. Am. Chem. Soc.* **1965**, *87*, 2945.

**TABLE 4.** Product Percent Yields from Photoreactions of 4–7 with NaOH by UV/Vis Analysis

reactant			
4	94%	3%	3%
5	70%	15%	15%
6	67%	17%	16%
7	61%	21%	18%

to those of 2-methoxy-5-nitrophenol and the 2-halo-4-nitrophenols. The spectrum at completion of each photoreaction was matched by iteration with variable compositions of three photoproducts totaling 100%. The results are in Table 4. It may be noted that these results are very close to those above for compounds 4–6 and slightly different for the minor products from 7. We have greater confidence in the UV/vis analyses and have used those results in the kinetic analyses.

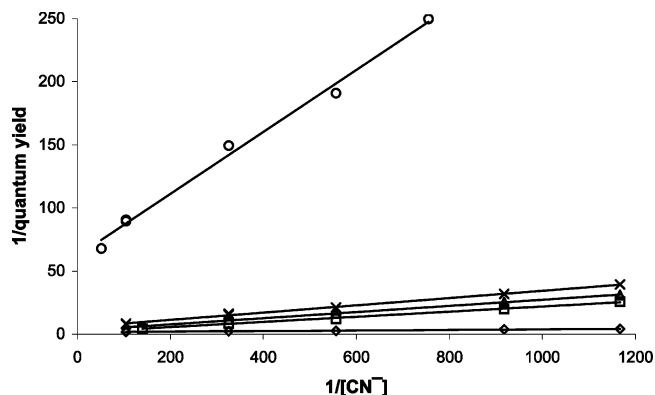
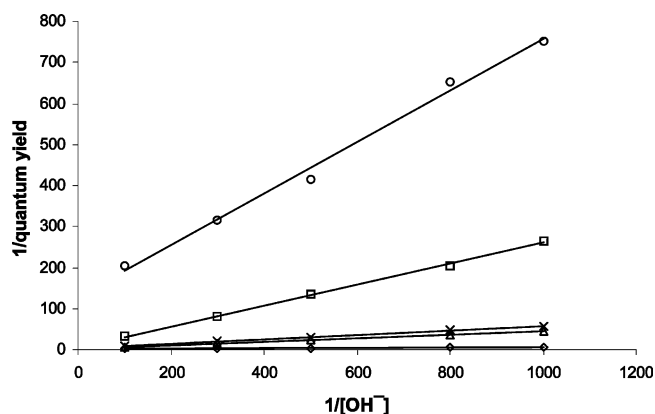
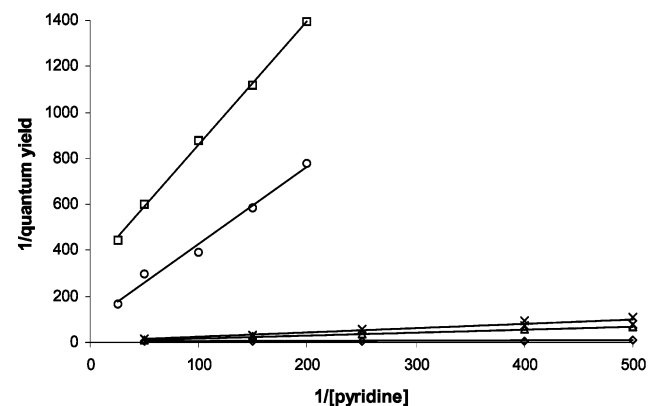
The photoreaction of pyridine with **1** in aqueous media is reported<sup>23</sup> to give exclusively displacement of nitrite ion, producing a pyridinium nitrite salt, and with **6** to give exclusively displacement of bromide, producing a pyridinium bromide salt.<sup>24</sup> We confirmed these findings for **1** and **6** for our irradiation conditions by NMR and by UV/vis. We found by UV/vis that compounds **4**, **5**, and **7** also photoreact cleanly to give the same pyridinium ion given by **6**.

Stern–Volmer plots of reciprocal quantum yield versus reciprocal nucleophile concentration were acquired with samples of **1** and **4–7** ( $2.2 \times 10^{-4}$  M) in quartz cuvettes in oxygen-free 33% CH<sub>3</sub>CN/H<sub>2</sub>O (v/v) with NaCN at 0.020–0.0010 M, NaOH at 0.010–0.0010 M, and pyridine at 0.040–0.0020 M. Cyanide ion concentrations were corrected for hydrolysis as if they were in pure water. Irradiation at 313 nm was carried out with a chromate filter with light from broadband 300 nm lamps. The photoreactions were followed to completion by overlaid UV scans to find a monitoring wavelength. Reactions were clean as shown by sharp isosbestic points and linear fraction of reaction with irradiation time through 10% reaction. Reaction extent was measured between 5 and 10% conversion; the actinometer was azoxybenzene in ethanol.<sup>25</sup> Plots of  $1/\Phi$  versus  $1/[\text{nucleophile}]$ , as shown in Figures 1–3, were linear. The slopes, intercepts, and limiting quantum yields at extrapolated infinite nucleophile concentration are given in Table 5.

Triplet lifetimes and yields were obtained in oxygen-free 33% CH<sub>3</sub>CN/H<sub>2</sub>O through use of a nanosecond transient spectrometer. The instrument utilized 8 ns pulses at 355 nm from a frequency-tripled Nd:YAG laser. Samples were contained in 1 cm quartz cuvettes, and the irradiation and monitoring beams were collinear. The triplet–triplet absorption maximum was established in each case near 400 nm and was used to monitor decay. The maximum optical density (OD) at the origin of the transient allowed estimation of the triplet yield with the assumptions that the triplet–triplet extinction coefficient was constant for each of the five compounds, and that the largest absorbance (for the chloride **5**) corresponded to a triplet yield

(24) Gamson, E. P. Ph.D. Dissertation, Northwestern University, 1970.

(25) Bunce, N. J.; LaMarre, J.; Vaish, S. P. *Photochem. Photobiol.* **1984**, *39*, 531.

**FIGURE 1.** Stern–Volmer plots for photoreactions of nitroisoles with NaCN in 33% acetonitrile/water:  $\diamond$  **4**;  $\square$  **1**;  $\Delta$  **5**;  $\times$  **6**;  $\circ$  **7**.**FIGURE 2.** Stern–Volmer plots for photoreactions of nitroisoles with NaOH in 33% acetonitrile/water:  $\diamond$  **4**;  $\square$  **1**;  $\Delta$  **5**;  $\times$  **6**;  $\circ$  **7**.**FIGURE 3.** Stern–Volmer plots for photoreactions of nitroisoles with pyridine in 33% acetonitrile/water:  $\diamond$  **4**;  $\square$  **1**;  $\Delta$  **5**;  $\times$  **6**;  $\circ$  **7**.

of 0.90. The basis for this assignment is that  $\Phi_{\text{ISC}}$  cannot exceed unity, and the highly efficient reactions of **1** and **4** with cyanide ion as measured by  $\Phi_{\text{lim}}$  (Table 5) are approximately equal to  $\Phi_{\text{ISC}}$  if the value for **5** is set at 0.9. The results are given in Table 6.

## Discussion

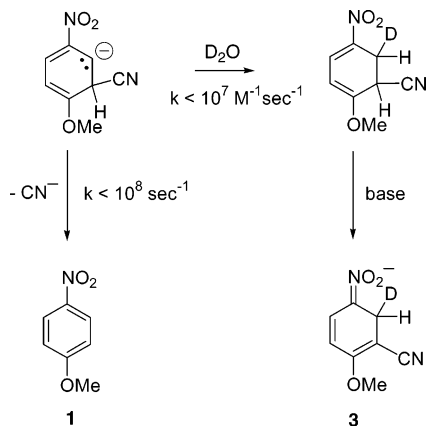
The production of **3** in high chemical yield and quantum yield from the photoreaction of **1** with cyanide ion can be rationalized by the sequence shown in Scheme 2. The  $\sigma$ -complex formed from the reaction of photoexcited **1** with cyanide ion would be

**TABLE 5.** Stern–Volmer Parameters for Photoreactions of Nitroanisoles with Cyanide Ion, Hydroxide Ion, and Pyridine

reaction	slope	intercept	intercept <sup>-1</sup> $\Phi_{lim}$
1 + CN <sup>-</sup>	0.020	1.6	0.62
4 + CN <sup>-</sup>	0.0023	1.6	0.62
5 + CN <sup>-</sup>	0.024	3.0	0.34
6 + CN <sup>-</sup>	0.029	5.6	0.18
7 + CN <sup>-</sup>	0.246	62	0.016
1 + OH <sup>-</sup>	0.26	6.0	0.17
4 + OH <sup>-</sup>	0.0051	1.9	0.54
5 + OH <sup>-</sup>	0.042	2.4	0.42
6 + OH <sup>-</sup>	0.055	3.6	0.28
7 + OH <sup>-</sup>	0.63	130	0.0077
1 + pyridine	5.4	325	0.0031
4 + pyridine	0.012	3.3	0.31
5 + pyridine	0.13	4.2	0.24
6 + pyridine	0.18	6.8	0.15
7 + pyridine	3.3	92	0.011

**TABLE 6.** Triplet Lifetimes, Decay Constants, and Yields of Nitroanisoles in 33% Acetonitrile–Water

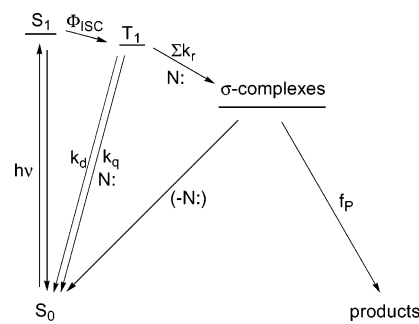
compound	lifetime (ns ± s.d.)	$k_d$ (s <sup>-1</sup> )	$T-T$ max OD at 400 nm	$\Phi_{ISC}$
1	58 ± 3	$1.7 \times 10^7$	0.053	0.69
4	217 ± 6	$4.6 \times 10^6$	0.048	0.62
5	137 ± 12	$7.4 \times 10^6$	0.069	0.90
6	116 ± 1.3	$8.6 \times 10^6$	0.064	0.84
7	44.5 ± 0.4	$2.2 \times 10^7$	0.031	0.40

**SCHEME 2.** Partitioning of the meta  $\sigma$ -Complex from Photoexcited 1 Plus Cyanide Ion

expected to be strongly basic (conjugate acid  $pK_a \cong 40$ ) yet would undergo deuteration relatively slowly. For a comparable system, a rate constant of  $5 \times 10^7 \text{ M}^{-1} \text{ s}^{-1}$  is reported for the protonation of toluene anion (conjugate acid  $pK_a \cong 41$ ) by water in THF.<sup>26</sup> The reaction rate would be slowed further in our case by an isotope effect. This implies that cyanide ion has the opportunity to depart from the  $\sigma$ -complex. This must not occur appreciably, however, in view of the high chemical and quantum yields of **3**. Cyanide ion, unlike most other nucleophiles, is sufficiently sticky to make a persistent complex that undergoes protonation (deuteration) on carbon to make a dihydrobenzene.<sup>27</sup> The dihydrobenzene has an acidic vinylogous  $\alpha$ -nitro proton that is also an  $\alpha$ -cyano proton. It should have a  $pK_a \cong 7$  and

(26) Dorfman, L. M.; Sujdak, R. J.; Bockrath, B. *Acc. Chem. Res.* **1976**, *9*, 352.

(27) We are not the first to discover that cyanide ion makes persistent addition complexes with aromatic substrates; see: Bunnett, J. F.; Zahler, R. E. *Chem. Rev.* **1952**, *52*, 273.

**SCHEME 3.** General Mechanistic Scheme for Nucleophilic Aromatic Photosubstitution

should be readily lost to make **3**. This implies that any  $\sigma$ -complexes made by attack of cyanide ion are unlikely to decay appreciably to starting materials by loss of cyanide and, therefore, that the fraction of each cyanide  $\sigma$ -complex that makes a detectable product is approximately unity.

A plausible mechanistic scheme for this reaction system is given in Scheme 3. Evidence from the literature<sup>13–16</sup> and from our flash photolysis experiments indicates that photoexcitation of **1** and **4–7** populates the triplet state quite efficiently. We consider first the case of the photochemistry with cyanide ion because of the simplification that the product yields should reflect the yields of intermediate  $\sigma$ -complexes, that is,  $f_P \cong 1$  for each product. Equations 1–3 can be derived readily for the reaction system. Equation 1 predicts the linear Stern–Volmer

$$\frac{1}{\Phi_x} = \frac{1}{\Phi_{ISC}} \left( 1 + \frac{k_q}{\sum k_r} + \frac{k_d}{\sum k_r [\text{CN}^-]} \right) \quad (1)$$

$$\text{slope} = \frac{1}{\Phi_{ISC}} \left( \frac{k_d}{\sum k_r} \right) \Rightarrow \sum k_r = \frac{1}{\Phi_{ISC}} \left( \frac{k_d}{\text{slope}} \right) \quad (2)$$

$$\text{intercept} = \frac{1}{\Phi_{ISC}} \left( 1 + \frac{k_q}{\sum k_r} \right) \quad (3)$$

plots, and the values from Tables 5 and 6 allow calculation of  $\sum k_r$  and  $k_q$ . The individual rate constants in  $\sum k_r$  can be extracted from the sum with the assumption that the yields of products in Table 1 are proportional to the nucleophilic attack rate constants that give their precursor  $\sigma$ -complexes. Rate constants for several of the elementary processes of this system are reported in Table 7.

The hydroxide ion reactions require one adjustment. The  $\sigma$ -complexes for displacement of halide ion and nitrite ion would not be expected to partition appreciably back to starting material since hydroxide ion (conjugate acid  $pK_a = 15.7$ ) is a much poorer leaving group than nitrite ion (conjugate acid  $pK_a = 3.4$ ) or the poorest leaving halogen, fluoride ion (conjugate acid  $pK_a = 3.5$ ). The yields of the halide and nitrite displacement products, therefore, should reflect the  $\sigma$ -complex precursor populations. The methoxide displacement, however, would have hydroxide ion loss competing with methoxide ion loss. Since these are comparable leaving groups, we assume that the yield of methoxide-substituted product represents half of the precursor  $\sigma$ -complex, which requires a corresponding adjustment of the relevant rate constant. This assumption and those described for cyanide ion yield the elementary rate constants for the hydroxide reactions in Table 8.

TABLE 7. Rate Constants of Cyanide Ion Processes with Triplet Nitroanisoles

reactant	$\Sigma k_r$ $10^9 \text{ M}^{-1} \text{ s}^{-1}$	$k_q$ $10^9 \text{ M}^{-1} \text{ s}^{-1}$	$k_{\text{nitro}}$ $10^9 \text{ M}^{-1} \text{ s}^{-1}$	$k_{\text{m-c}}$ $10^9 \text{ M}^{-1} \text{ s}^{-1}$	$k_X$ $10^9 \text{ M}^{-1} \text{ s}^{-1}$	$k_X$ relative
<b>1</b>	1.2	0.15	0.29	0.89	n.a.	
<b>4</b>	3.3	0.011	0.29	0.081	2.9	27
<b>5</b>	0.34	0.56	0.098	0.034	0.21	1.9
<b>6</b>	0.36	1.3	0.11	0.039	0.20	1.9
<b>7</b>	0.22	5.4	0.096	0.020	0.11	1.0

TABLE 8. Rate Constants of Hydroxide Ion Processes with Triplet Nitroanisoles

reactant	$\Sigma k_r$ $10^9 \text{ M}^{-1} \text{ s}^{-1}$	$k_q$ $10^9 \text{ M}^{-1} \text{ s}^{-1}$	$k_{\text{nitro}}$ $10^9 \text{ M}^{-1} \text{ s}^{-1}$	$k_{\text{OMe}}$ $10^9 \text{ M}^{-1} \text{ s}^{-1}$	$k_X$ $10^9 \text{ M}^{-1} \text{ s}^{-1}$	$k_X$ relative
<b>1</b>	0.095	0.29	0.076	0.032	n.a.	
<b>4</b>	1.4	0.24	0.043	0.084	1.3	29
<b>5</b>	0.20	0.22	0.029	0.025	0.12	2.6
<b>6</b>	0.19	0.38	0.032	0.028	0.11	2.4
<b>7</b>	0.087	4.5	0.018	0.016	0.045	1.0

TABLE 9. Rate Constants for Pyridine Processes with Triplet Nitroanisoles

reactant	$\Sigma k_r$ $10^9 \text{ M}^{-1} \text{ s}^{-1}$	$k_q$ $10^9 \text{ M}^{-1} \text{ s}^{-1}$	$k_{\text{nitro}}$ $10^9 \text{ M}^{-1} \text{ s}^{-1}$	$k_X$ $10^9 \text{ M}^{-1} \text{ s}^{-1}$	$k_X$ relative
<b>1</b>	0.0046	1.0	0.0046	n.a.	
<b>4</b>	0.63	0.67		0.63	39
<b>5</b>	0.063	0.18		0.063	3.9
<b>6</b>	0.057	0.27		0.057	3.5
<b>7</b>	0.016	0.59		0.016	1.0

Partitioning of  $\sigma$ -complexes at the halogen-bearing carbon back to starting materials for the photosubstitutions by pyridine (conjugate acid  $\text{p}K_a = 5.3$ ) seems unlikely for Cl, Br, and I, the anions of which all have conjugate acid  $\text{p}K_a$  values of  $-7$  or below and should be relatively fast leaving groups. Partitioning back to starting materials could occur for the displacements of nitrite ion from **1** (conjugate acid  $\text{p}K_a = 3.4$ ) and fluoride ion from **4** (conjugate acid  $\text{p}K_a = 3.5$ ). Reversion seems likely, however, to be a minor process in each case, and we have at this time no basis for assessing it. We have assumed no partitioning of  $\sigma$ -complex intermediates back to starting materials for the elementary rate constants for the pyridine reactions summarized in Table 9.

The rate data in Tables 7–9 display a wealth of subtle effects of structural changes in these reactions. The nitro group displacements ( $k_{\text{nitro}}$ ) would be expected to be little affected by meta substituents, and indeed the rate constants for attack on **1** and **4–7** leading to nitrite displacement are within a factor of 3–4 for cyanide ion and for hydroxide ion. For these displacements, the cyanide ion rate constants are 3.5–7 times faster than those of hydroxide ion and 63 times faster than that of pyridine for the one comparison available. These nucleophilicities compare surprisingly closely with an averaged nucleophilicity measure for aqueous solution with saturated carbon substrates for which cyanide ion reacts about 4 times faster than hydroxide ion and 31 times faster than pyridine.<sup>28</sup> Similarly, the rates of bond formation at the unsubstituted meta carbon by cyanide ion would be expected to be modestly affected by halogens at the meta position, and they are within a factor of 4. That this rate constant for **1** is about 10 times greater than that of **4** may reflect its statistical advantage of two meta positions and other unknown effects of having no halogen on the ring. The ratio of rate constants for nitro versus meta carbon attack

by cyanide ion is steady in the range of 3–5 for **4–7**, as would be expected. The comparable ratio for nitro versus methoxy attack by hydroxide ion is also quite steady for the halogen series in the range of 0.5–1.

Since little is known about nucleophile-induced quenching mechanisms, we note only a few highlights. The quenching by cyanide ion correlates with the polarizability expected for the nitroaromatic compounds. The rates of quenching of the iodide by cyanide ion and hydroxide ion are at or above the rate of diffusion, and these account for the great inefficiency of photoproduct formation from **7** ( $\Phi_{\text{lim}} = 0.016$  and 0.0077, respectively). These contrast especially with the cyanide ion reactions of **1** and **4**, which show slow quenching and whose limiting quantum yields ( $\Phi_{\text{lim}} = 0.62$  and 0.62) are approximately the same as the estimated quantum yields of intersystem crossing. That the quenching by hydroxide ion occurs at a fairly constant rate for **1** and **4–6** and does not correlate with polarizability may stem from a quenching possibility that hydroxide ion has and cyanide ion does not have. Nucleophilic attack at an unsubstituted meta carbon by cyanide ion generates a photoproduct, but the corresponding hydroxide ion  $\sigma$ -complex would lose hydroxide ion, resulting in quenching. The quenching by pyridine also does not vary systematically with halogen substitution and, except for the iodide, is similar in size to that of hydroxide ion. This suggests that pyridine also quenches by the nucleophilic attack process described above for hydroxide ion. These findings are similar to those of Letsinger and McCain<sup>21a</sup> for a related system.

Our major interest is in the rate constants for the attack of nucleophiles at the halogen-bearing carbon. The rate for excited fluoride **4** plus cyanide ion is at the diffusion limit, which for water is reported for non-lyate reactants having no ionic attraction or repulsion to be  $3 \times 10^9 \text{ M}^{-1} \text{ s}^{-1}$ .<sup>29</sup> The rate ratios for F/Cl/Br/I are 27:1.9:1.9:1, respectively. The fastest rate for hydroxide ion is about half the rate of diffusion, and the relative rates for F/Cl/Br/I are 29:2.6:2.4:1, respectively. The fastest rate for pyridine is about one-fifth of the rate of diffusion, and the relative rates for F/Cl/Br/I are 39:3.9:3.5:1, respectively. All of these element effects follow the pattern of aromatic substitution<sup>8,9</sup> and not aliphatic substitution or elimination,<sup>7</sup> implying that carbon–nucleophile bond formation not carbon–halogen

(28) Wells, P. R. *Chem. Rev.* **1963**, 63, 171.(29) (a) Eigen, M. *Angew. Chem., Int. Ed. Engl.* **1964**, 3, 1. (b) Weller, A. Z. *Phys. Chem.* **1958**, 17, 224.

bond fission is the principal efficiency-determining process. These findings, like those for the famous thermal case,<sup>8</sup> provide strong evidence against a concerted mechanism or any other mechanism involving C–X bond fission in the efficiency-determining step. They support efficiency-determining intermediate  $\sigma$ -complex formation.

The thermal substitutions of 1-halo-4-nitrobenzenes with sodium methoxide in methanol show relative rates of halogen displacement of 1300:3:2:1 for F/Cl/Br/I, respectively, the iodide having a rate constant of  $1.3 \times 10^{-7} \text{ M}^{-1} \text{ s}^{-1}$ .<sup>30</sup> This reaction series is comparable to our photochemical series in using a simple hard atom nucleophile in a protic solvent. Since the photoreaction of fluoride **4** with cyanide ion is diffusion-controlled, the intrinsic energy barrier of the reaction is 0. The incremental Arrhenius activation energy barriers for Cl, Br, and I are 1.6, 1.6, and 1.9 kcal/mol for cyanide ion. For hydroxide ion, the increments of activation energy (vs the fluoride) for Cl, Br, and I are 1.4, 1.5, and 2.0 kcal/mol, respectively, and for pyridine, the corresponding increments are 1.4, 1.4, and 2.2 kcal/mol. For the thermal displacements by methoxide ion,<sup>30</sup> the increments of Arrhenius activation energy relative to the fluoride (for Cl, Br, and I) are 3.6, 3.8, and 4.2 kcal/mol. Thus, despite absolute rate differences on the order of  $10^{14}$ , the thermal and the photochemical reaction series show comparable halogen element effects and barrier increments. The element effect in the photoreaction is damped in rate by roughly a factor of 40, or about 2 kcal/mol in incremental activation energy. This strongly suggests that the photoreaction, like the vastly slower thermal one, must involve simple electron-paired bond formation with its attendant local van der Waals repulsion and  $\sigma$ -bond polarization effects of the attached halogen.

The nucleophilicities evident in the halogen photosubstitutions are similar to those for the comparatively slow thermal substitutions. Cyanide ion attacks the halogen-bearing carbons 1.8–2.4 times faster than hydroxide ion does and 3.3–6.9 times faster than pyridine does. For aqueous solution with saturated carbon substrates, cyanide ion reacts on average about 4 times faster than hydroxide ion and 31 times faster than pyridine,<sup>28</sup> that being a range of 2 kcal in incremental activation energy. Thus nucleophilicities, like the element effects, in the photoreactions are damped in rate by roughly a factor of 6, or about 1 kcal/mol in incremental activation energy. Again, the remarkable similarity of local effects despite the huge difference in rates suggests that the transition states are similar, namely, electron-paired formation of a bond through nucleophilic attack. That the behavior of pyridine is so similar to that of hydroxide ion and cyanide ion suggests, moreover, that the powerful forces of solvation and desolvation for the ions (that would be much diminished for neutral pyridine) do not appear in the relative rates.

It may be noted that our sparse data on nucleophilicities for attack at the nitro-bearing carbon show a similar picture. They span a range of about 60 in rate (pyridine/hydroxide ion/cyanide ion all for **1** are 1:17:63) that is 2-fold larger than that for the thermal reactions of these nucleophiles. This corresponds, however, to only 2.5 kcal in incremental activation energy difference, which is close to the 2.0 kcal range for the thermal case. This also argues that the transition state leading to the  $\sigma$ -complex for nitro displacement is, at the local level, sterically

and electronically similar to that of ground state nucleophilic transition states.

Attempts to understand the  $S_N2Ar^*$  mechanism proceeding from a triplet  $\pi, \pi^*$  state have a long history.<sup>1,5</sup> The regiochemical and reactivity questions are embedded in the reaction of a singlet nucleophile with a triplet excited aromatic substrate. The reaction proceeds with a large energy release to form energetic, singlet intermediates before reaching the singlet products. The sequence is a classical problem in photochemical mechanisms<sup>31</sup> that has been only slightly elucidated despite extensive study. Our results shed some new light on this mechanism.

The theory of Epiotis and Shaik<sup>11</sup> predicts regioselectivity in  $S_N2Ar^*$  reactions based on frontier molecular orbital theory. It postulates that reaction will be favored at ring carbon atoms having a maximal ground state HOMO coefficient and a minimal ground state LUMO coefficient. Semiempirical calculations (AM1) in Spartan '04 reveal that the maximum of the difference of absolute value of the HOMO coefficient minus absolute value of the LUMO coefficient predicts the major product in each case reported here. In most cases, however, the yields of minor products do not correlate with the coefficient differences. It should be noted that prediction of the major products for these cases is not risky and furnishes little validation of the theory. It would do as well to predict simply that maximum detectable reaction occurs meta to the nitro group, and it appears that the maximum ground state coefficient difference serves merely to identify that position. Indeed, this theory seems to us to lack justification since it postulates excited-state regioselectivity based on orbitals that do not exist in the reacting excited molecules. The model is based on purported properties of the initial state, a known weakness in predicting regioselectivity in aromatic substrates.<sup>32</sup> Moreover, the reacting molecules are not of the same multiplicity as the molecules calculated. The argument<sup>11</sup> that the triplet should react like the excited singlet because spin–orbit coupling would be large and would convert the triplet encounter complex to a singlet encounter complex before forming the singlet  $\sigma$ -complex seems wholly without justification for the cases reported here. Despite its success for the major products, we do not believe that the Epiotis–Shaik model provides a satisfactory rationale for the regioselectivity and reactivity of  $S_N2Ar^*$  reactions.

The other extant rationale of regioselectivity of  $S_N2Ar^*$  reactions was put forward by van Riel, Lodder, and Havinga.<sup>12</sup> It postulates that the energy gap law for radiationless electronic transitions, that is, that internal conversions between states close in energy are faster than those between states far apart in energy, should apply to the selection of favorable transition states for photosubstitution. Since singlet meta-to-nitro  $\sigma$ -complexes or those for displacement of the nitro group are little stabilized by resonance, they are much less stable than the ortho or para  $\sigma$ -complexes. Thus the transition from the triplet encounter complex to the less stable (meta)  $\sigma$ -complexes was judged<sup>12</sup> to be faster than that of the more stable (ortho or para)  $\sigma$ -complexes. This model also successfully rationalizes the products of the reactions reported here, although it cannot distinguish major from minor products among those products favored by the model.

(31) Havinga, E. *Reactivity of the Photoexcited Molecule*; Wiley: New York, 1967; p 201.

(32) Dewar, M. J. S. *The Molecular Orbital Theory of Organic Chemistry*; McGraw-Hill: New York, 1969; Chapter 6.

(30) Bartoli, G.; Todesco, P. E. *Acc. Chem. Res.* **1977**, *10*, 125.

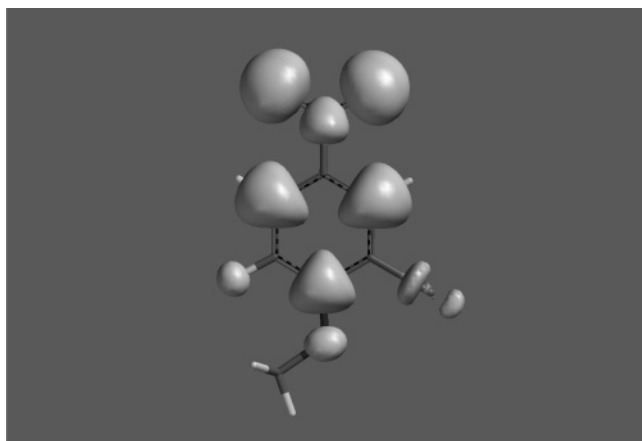
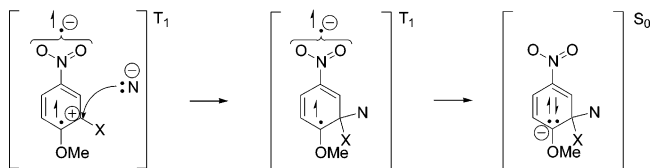


**FIGURE 4.** Odd electron spin distribution in triplet 2-chloro-4-nitroanisole by Hartree–Fock calculation using a 3-21G\* basis set.

Certain details of the formulation of this model lead us to question its applicability to the reactions reported here. The energy gap law applies most strongly to internal conversion processes in which the states have the same multiplicity, which is not the case here. Moreover, the states involved in an electronic internal conversion that might be energy gap controlled must be of sufficiently similar geometries that their electronic surface wells align with each other and do not have a surface intersection at low energy levels of the lower state. If they are offset, a surface crossing can occur at easily accessible vibrational levels that would sidestep low probability, energy-forbidden processes. Offset of energy wells seems likely to be the case for the reactions reported here because the geometries of the upper and lower states differ substantially. Moreover, the suggestion<sup>12</sup> that the energies of the triplet  $\sigma$ -complexes, whose energies were estimated by CNDO/2 calculations, should represent the energies of the triplet encounter complexes seems questionable.

The key to understanding the regiochemistry of these reactions may lie in a little noticed result of van Riel, Lodder, and Havinga,<sup>12</sup> namely, that the triplet meta  $\sigma$ -complexes of nitrophenyl ethers with methoxide ion or hydroxide ion are about 14 kcal/mol more stable than the triplet para  $\sigma$ -complexes, as indicated by CNDO/2 calculations. While we do not know at this time the energy of the triplet aromatic–nucleophile encounter complex, the result implies that conversion from a triplet aromatic–nucleophile encounter complex to a triplet  $\sigma$ -complex may be more endothermic or less exothermic for a para  $\sigma$ -complex than for a meta  $\sigma$ -complex. A suggestion of why this might be so is indicated in Figure 4, which shows that the odd electrons in the triplet of 2-chloro-4-nitroanisole are distributed in the ring entirely at C<sub>1</sub>, C<sub>3</sub>, and C<sub>5</sub>, and not at all at C<sub>2</sub>, C<sub>4</sub>, and C<sub>6</sub>, the positions most susceptible to nucleophilic attack. Very similar results for the odd electron distribution were obtained for all of the triplet nitroanisoles in this study, whether the calculations were done by semiempirical methods (MINDO, AM1, or PM3) or by higher order calculations (Hartree–Fock with 3-21G\* or 6-31G\* basis sets, or by density functional methods). Inasmuch as the triplet  $\pi,\pi^*$  state can be represented as having the promoted electron in an antibonding orbital mostly on the nitro group and the electron hole mostly in the  $\pi$ -orbitals of the ring (a cation radical moiety), approach of a nucleophile to bond at C<sub>1</sub>, C<sub>3</sub>, or C<sub>5</sub> would be unfavorable initially because

**SCHEME 4.** Modified Valence Bond Depiction of Reaction of a Nucleophile with a Triplet  $\pi,\pi^*$  Excited State of a 2-Halo-4-nitroanisole



more electrons would be present at these positions than can be accommodated in a two-electron bond. Alternatively, approach of the nucleophile at C<sub>2</sub>, C<sub>4</sub>, or C<sub>6</sub> encounters cationic carbon, which should afford two-electron bond formation with little or no activation energy. Any activation energy required would reflect local substituent and nucleophile effects. This makes a very good summary of the facts we observe.

If  $\sigma$ -complex formation occurs within the triplet manifold, the reaction is an internal conversion process, but application of the energy gap law to this case predicts the wrong product since triplet meta  $\sigma$ -complexes appear to be much lower in energy than triplet para  $\sigma$ -complexes.<sup>12</sup> Moreover, application of the energy gap law would require intersystem crossing to be concerted with conversion from the triplet encounter complex to a singlet  $\sigma$ -complex. A further indication that this is not the mechanism may be seen from the absence of a spin–orbit coupling effect on the rates. We see relative rates of bond formation at the halogen-bearing carbon for F/Cl/Br/I of roughly 30:2:2:1. Since spin–orbit coupling is essential to rapid intersystem crossing, the relative rates should lie strongly in the opposite direction if intersystem crossing were involved because  $I \gg \text{Br} > \text{Cl} > \text{F}$  in spin–orbit coupling. These considerations seem to us to settle the question in favor of nucleophilic reaction occurring within the triplet manifold.

We envision nucleophilic attack on the triplet as shown in Scheme 4. The first structure is a modified valence bond depiction of the triplet  $\pi,\pi^*$  excited state of a halonitroanisole showing the promoted electron in an antibonding orbital mainly on the nitro group and the electron hole mainly in the  $\pi$ -orbitals of the ring. Electron-paired bond formation occurs within the triplet manifold. The product triplet  $\sigma$ -complex probably undergoes spin inversion quite rapidly to make the singlet  $\sigma$ -complex. This sequence is not quite the same as  $\sigma$ -bonding by the triplet plus nucleophile entering a funnel in the potential energy surface leading to the singlet  $\sigma$ -complex, a suggestion we had made earlier.<sup>10</sup> Electron-paired bond formation within the triplet manifold (that is, with no kinetic involvement of spin inversion) explains the astounding facts that the photochemical reactions show small local van der Waals and  $\sigma$ -bond polarization effects and nucleophilicity effects that are similar to those of ground state reactions despite being about  $10^{14}$  times faster. Reaction within the triplet manifold also explains why there is no observable spin forbiddenness in the diffusion-controlled reaction of fluoride **4**. The relatively unfavored displacement of the para methoxy group by hydroxide ion may result from some small endothermicity, or lower exothermicity, or reversibility that could result from the bond-forming reaction occurring within the triplet manifold, but this would not be spin forbiddenness. Electron-paired bonding of an excited triplet molecule



to a nucleophile appears to be analogous to a recently discovered electron-paired nucleophilic reaction of a para benzyne biradical.<sup>33</sup>

## Experimental Section

The 2-halo-4-nitroanisole photoreactants were prepared from the available 2-haloanisoles by nitration in 1:1 HNO<sub>3</sub>(70%)/HOAc by the method of Reverdin.<sup>34</sup> 2-Methoxy-5-nitrobenzotrile was prepared similarly. After recrystallization from ethanol–water, the melting points of these substances agreed with the literature values,<sup>35</sup> and they gave satisfactory <sup>1</sup>H NMR spectra. 4-Nitroanisole, 4-methoxyphenol, 4-nitrophenol, 4-methoxybenzotrile, 2-methoxy-5-nitrophenol, 3-bromo-4-methoxybenzotrile, and 3-chloro-4-methoxybenzotrile were commercial substances whose <sup>1</sup>H NMR spectra matched those of any corresponding photoproducts. The pyridinium salt from **1** has been reported,<sup>23</sup> as has that from **6**.<sup>24</sup> We confirmed the pyridinium salts from **4–7** principally from the coincidence of the UV/vis spectra of our photoreactions at completion ( $\lambda_{\text{max}} = 300 \text{ nm}$ ,  $\epsilon = 10\,900$  in 33% acetonitrile/water) with the spectrum reported<sup>24</sup> ( $\lambda_{\text{max}} = 301 \text{ nm}$ ,  $\epsilon = 12\,000$  in 10% *t*-butyl alcohol/water). We also confirmed the pyridinium salt from **1** and that from **6** by their NMR spectra, which were as expected. The 3-halo-4-methoxybenzotriles that are minor products from the cyanide ion photoreactions were identified in solution by their <sup>1</sup>H NMR spectra, which were similar to each other and were as expected. The chloride and bromide were confirmed directly with authentic samples. The nitronate ion photoproduct that is the major product from **1** with cyanide ion was identified by NMR and by oxidation with 3,5-dinitrobenzoic acid, as described in Results. The nitronate ions that are minor products from the cyanide ion photoreactions with **4–7** were identified in solution also by their <sup>1</sup>H NMR spectra, especially the upfield-shifted methoxy signal. One of these, formed in low yield from chloride **5**, was confirmed by oxidizing the photoproducts in solution in an NMR tube with 3,5-dinitrobenzoic acid, which caused replacement of the nitronate ion peaks with those assignable to the aromatized substance, 3-chloro-2-methoxy-5-nitrobenzotrile. An example of a <sup>1</sup>H NMR spectrum used for product analysis of the photoreaction of **5** with cyanide ion is included in the Supporting Information.

The minor products from the hydroxide ion photoreactions include the 2-halo-4-nitrophenols and the 3-halo-4-methoxyphenols. The former were characterized by NMR and UV/vis. Samples of **4–7** (0.010 M) and NaOD (0.10 M) in 25% DMSO-*d*<sub>6</sub>/D<sub>2</sub>O were heated in NMR tubes at 80 °C, and the thermal hydrolysis of the methoxy group, as shown by quantitative production of methanol, was followed in each case by periodic observation of the spectrum. The reactions were clean with half-lives on the order of 10 h. The 2-halo-4-nitrophenol anion was the other product in each case. Each of these gave the expected NMR spectrum, with the exception that substantial or complete deuterium exchange occurred at C-3. The product solutions at completion were diluted quantitatively in 33% CH<sub>3</sub>CN–H<sub>2</sub>O to obtain the UV/vis spectra of the anions, all of which showed the expected  $\lambda_{\text{max}}$  near 400 nm,  $\epsilon = \text{ca. } 19\,000$  (see below).

3-Bromo-4-methoxyphenol and its sodium salt were prepared in solution by adding bromine to 4-acetoxyanisole followed by alkaline hydrolysis of the ester. The NMR spectra were as expected. That of the anion matched the NMR spectrum of one of the minor products of the photolysis of **6** with NaOH and closely matched the NMR spectra of the other 3-halo-4-methoxyphenoxides that are minor products of the photolyses of **4**, **5**, and **7**. An NMR spectrum of a photoproduct mixture from the photolysis

of **5** with NaOH that is typical of those used for NMR product analyses of the hydroxide ion reactions is in the Supporting Information.

The requisite extinction coefficients at relevant wavelengths in 33% CH<sub>3</sub>CN–H<sub>2</sub>O for the UV–vis product analyses of photolyses of **4–7** with NaOH are in Table 3. The spectrum of each photoproduct mixture was analyzed at completion of photolysis, which was done with chromate-filtered light (313 nm) from broad-band 300 nm lamps in 1.0 cm cuvettes. Completion was determined by UV/vis spectral overlays for reactions at  $1.0 \times 10^{-4}$  M starting material and 0.010 M NaOH. The reactions all showed sharp isosbestic points and were analyzed by iteration for composition of the three types of products at wavelengths of 405, 323, and 265 nm assuming that the sum of the concentrations was  $1.0 \times 10^{-4}$  M. The small extinctions of sodium 4-methoxyphenoxide were taken to represent those of the sodium 3-halo-4-methoxyphenoxides and their unknown photohydrolysis products. Because the extinctions are small, the method essentially estimates the yields of 3-halo-4-methoxyphenoxides by difference based on the more intensely absorbing nitrophenoxides.

Photolyses for NMR analyses of products were carried out in borosilicate NMR tubes with unfiltered radiation from 300 nm broad-band lamps (Rayonet RPR-208) with starting material concentrations of about 0.005 M and nucleophile concentrations of about 0.01 M. Solutions were not freed of oxygen except for the cyanide ion cases, which were bubbled out with argon. Photolyses for determination of quantum yields were carried out in 1.0 cm septum-closed quartz cuvettes with starting materials at  $2.2 \times 10^{-4}$  M in 33% CH<sub>3</sub>CN–H<sub>2</sub>O. Solutions were freed of oxygen by bubbling with argon. The concentration of NaCN ranged from 0.020 to 0.0010 M; that of NaOH was 0.010 to 0.0010 M; and that of pyridine was 0.040 to 0.0020 M. The concentration of cyanide ion was corrected for hydrolysis as if it were in pure water. Irradiation at 313 nm was carried out in the Rayonet chamber with 300 nm lamps by suspending the cuvette in a quartz well containing approximately a 1 cm path on all sides of aqueous 0.002 M K<sub>2</sub>CrO<sub>4</sub> containing 5% Na<sub>2</sub>CO<sub>3</sub>. The samples were approximately optically opaque at 313 nm. Reactions were followed to completion by making spectral overlays (200–600 nm) for reaction at an intermediate nucleophile concentration to find an appropriate wavelength for quantitative analysis. The reactions were clean as judged by sharp isosbestic points. The progress was linear with time of irradiation through at least 10% reaction, and they were analyzed between 5 and 10% of completion. The actinometer was azoxybenzene in ethanol,<sup>25</sup> and typical absorbed light intensity was  $2.87 \times 10^{-6}$  einsteins/L/s.

Nanosecond transient absorption spectroscopy was carried out with samples in oxygen-free 33% CH<sub>3</sub>CN–H<sub>2</sub>O in 1.0 cm quartz cuvettes. Samples of **1** and **4–7** with an optical density of about 0.5 at 355 nm were excited with 8 ns, 2.8 mJ, 355 nm pulses from frequency-tripled output of a Nd:YAG laser. The excitation pulse was directed to a 5 mm diameter spot matched collinearly to the probe pulse from a xenon flashlamp. The probe pulse was detected by passing it through a monochromator to a photomultiplier tube whose output terminated in a fast storage oscilloscope. About 100–150 kinetic traces taken over several minutes were averaged at each of 4–6 wavelengths between 390 and 415 nm to determine the wavelength maximum of the transient and its decay kinetics. The spectra are attributable to a triplet–triplet absorption. Analysis of the kinetic data was performed with a Levenberg–Marquardt nonlinear least-squares fit to a general sum-of-exponentials function with an added Gaussian to account for the instrument response time of about 8 ns. Determination of the maximum optical density of the transient was done manually by inspecting the OD versus time output at each of the wavelengths investigated. The triplet lifetime in each case is an average of 4–9 determinations, each representing an average of 100–150 kinetic traces.

Molecular orbital calculations were carried out with Spartan '04, version 1.0.3, software running on a desktop computer. Semiemp-

(33) Perrin, C. L.; Rodgers, B. L.; O'Connor, J. M. *J. Am. Chem. Soc.* **2007**, *129*, 4795.

(34) Reverdin, F. *Chem. Ber.* **1896**, *29*, 2598.

(35) *Dictionary of Organic Compounds*; Pollock, J. R. A., Stevens, R., Eds.; Oxford: New York, 1965; Vols. 1–3.

pirical AM1 calculations were used for most cases, but higher level calculations of Hartree–Fock or density functional type with 3-21G\* or 6-31G\* basis sets were used to check on the accuracy of the AM1 calculations.

**Acknowledgment.** This paper is dedicated to Joseph F. Bunnett on the occasion of his 86th birthday. Acknowledgement is made to the donors of the Petroleum Research Fund, administered by the American Chemical Society, for support of this work. We thank Amy Vega and Prof. Michael Wasielews-

ki of Northwestern University for the transient measurements. We thank Dr. Albert Stolow for a discussion of the energy gap law.

**Supporting Information Available:** <sup>1</sup>H NMR spectrum supporting Scheme 1, typical <sup>1</sup>H NMR spectra for product analyses of NaCN, NaOH, and pyridine photoreactions, a typical transient decay curve, and calculated details for Figure 4. This material is available free of charge via the Internet at <http://pubs.acs.org>.

JO702468D